Cold Regions Science and Technology 153 (2018) 172–180

Contents lists available at ScienceDirect

Cold Regions Science and Technology

journal homepage: www.elsevier.com/locate/coldregions

Joint studies of water phase transitions in Na-bentonite clay by calorimetric and dielectric methods

V.L. Mironov[a], A.Yu Karavayskiy[a,*], Yu.I. Lukin[a], E.I. Pogoreltsev[a,b]

[a] Kirensky Institute of Physics, Federal Research Center KSC SB RAS, 660036 Krasnoyarsk, Russia
[b] Krasnoyarsk, Russia Institute of Engineering Physics and Radioelectronics, Siberian State University, Krasnoyarsk 660074, Russia

ARTICLE INFO

Keywords:
Frozen soil
Non-freezing water
Unfrozen water
Bound water
Phase transitions
DSC
Dielectric permittivity
Dielectric model

ABSTRACT

The present study consisted of an experimental investigation of phase transitions of soil water contained in moist Na-bentonite clay, using the differential scanning calorimetry (DSC) method, within the temperature range from −40 to 20 °C. Based on the results of DSC analysis, the following components of soil water were found in the frozen bentonite: non-freezing water, unfrozen water and ice. The proposed method of processing the obtained experimental calorimetric data allowed us to determine the temperature dependencies of the content of particular soil water components. Latent heat of fusion was found in two cases, namely: where the ice was transformed into bound or unbound unfrozen soil water. The results of the investigation into phase transitions, obtained via calorimetric measurements, were used to substantiate the method for studying the phase transitions of soil water by dielectric measurements. With this in mind, complex relative permittivity testing was conducted on the same moist Na-bentonite clay, in the temperature range from −30 to 0 °C and a gravimetric moisture range from the dry soil to 1 g/g. Based on the results of these dielectric tests and a refractive dielectric mixture model (RDMM), the following components of water were identified in the frozen soil: tightly bound water, loosely bound water, unbound water and ice. The dependences of the content of these components of soil water on the temperature were calculated. It was shown that the increase in the mass of unfrozen loosely bound water, as a result of a decrease in the ice mass, determined with dielectric measurements, is quantitatively consistent with the dependence calculated using calorimetric testing. This proves that the changes of the mass of the loosely bound water, determined by dielectric measurements, is a result of the phase transition and the corresponding temperature dependence can be used to determine the characteristics of these phase transitions.

1. Introduction

The existing knowledge about phase transitions of water in frozen soils is described in monographs (Yershov and Williams, 2004; Frolov, 1998) as well as in works published more recently (Kozlowski, 2003a,b, 2007; Wu et al., 2008). According to the concepts described in these works, frozen soils contain some amount of liquid water, referred to as unfrozen water. It is believed that frozen soil contains both unfrozen water and ice. As the temperature of the frozen soil decreases, the content of unfrozen water is gradually reduced as water becomes ice. This principle of phase transition of the water in soils is predominant in contemporary sources (Kozlowski, 2003a,b, 2007; Osipov, 2012). It is considered (Frolov, 1998), that unfrozen water found in frozen soils is physically bound, adsorbed on the solid surface. Bound water is usually divided into tightly and loosely bound water (Frolov, 1998; Wu et al., 2008; Kozlowski, 2003a,b). The frozen grounds and soils almost always contain unfrozen water, which at a fixed state (at a constant temperature) is in thermodynamic equilibrium with ice, in contrast to unbound liquid water. Unbound water in thawed and frozen soils can be either in liquid form or in the form of ice. This is not supercooled water, but a special liquid phase, which, below the freezing point, crystallizes into ice at a lower temperature (Tsytovich, 1975). Unfrozen water is one of the important components of moist frozen soils, that defines the value of its permittivity. The content of unfrozen water in frozen soil affects the soil dielectric permittivity, being an important parameter in the construction of dielectric models of frozen soil. Some works (Kozlowski, 2003a,b; Kozlowski and Nartowska, 2013) talk of the existence of non-freezing and unfrozen water in frozen clay. Some literature (Frolov, 1998) states that unfrozen water is found in a bound state. This water, as shown in Mironov et al. (2017), has its own permittivity as a function of temperature, unfrozen water is the water that is not in a state of ice, it is present both in freezing and thawing soils. According to the results obtained through the work described earlier, several water components can be present in frozen soil:

* Corresponding author.
E-mail addresses: rsdvm@ksc.krasn.ru (V.L. Mironov), rsdak@ksc.krasn.ru (A.Y. Karavayskiy), rsdlu@ksc.krasn.ru (Y.I. Lukin), pepel@iph.krasn.ru (E.I. Pogoreltsev).

https://doi.org/10.1016/j.coldregions.2018.04.010
Received 29 May 2017; Received in revised form 13 April 2018; Accepted 16 April 2018
Available online 05 June 2018
0165-232X/

1. unbound water, which can be in liquid form in thawed soil or ice in frozen soil, usually become frozen at 0 °C, or in high temperature areas at negative temperatures close to 0 °C in the case of unsalted or slightly saline soils;
2. loosely bound water, which is unfrozen liquid water, found in thawed and frozen soils, whilst in the latter, with decreasing temperature, within a finite range of temperature the loosely bound water gradually transforms into ice;
3. tightly bound water (non-freezing water), which is water, consisting of molecules adsorbed on the surface of mineral particles, in both frozen and in thawed soils, which, in some studies (Bogdan et al., 1996; Turov and Leboda, 1999; Gun'ko et al., 2008; Kozlowski, 2011) was observed in the unfrozen state at the temperatures down to −70 °C.

This classification for various components of soil water existing in frozen and thawed soil was introduced in Wu et al. (2008). Such classification is used as a simplification that is convenient in formulation of the refractive dielectric model of the mixture. The concept of this classification of water components is schematically presented in Wu et al. (2008) in Fig. 1.4. Taking into account the classification of water in the soil considered above, we conclude that all unfrozen water in frozen soil, present both freezing and thawing soils, consists of tightly bound and loosely bound water.

The following four methods are usually used in the experimental investigation to determine the content of unfrozen water depending on the temperature:

1. calorimetry (Williams, 1964; Frivik and Johansen, 1978);
2. differential scanning calorimetry (Kozlowski, 2003a,b, 2007);
3. nuclear magnetic resonance (NMR) (Watanabe and Mizoguchi, 2002);
4. dielectric spectroscopy (Fabbri et al., 2006, 2009; He and Dyck, 2013; He et al., 2016).

All these methods rely on the belief that phase transitions of unfrozen water to ice continues in indefinitely small portions as the temperature gradually decreases. In all these studies, the dependence of the arising ice as a function of temperature was measured, and the mass of unfrozen water was determined as the difference between the total content of water in the sample and the mass of ice. Thus, within the general classification, the sum of the total content of loosely bound and tightly bound water was measured. The content of non-freezing tightly bound water was first determined in a study (Kozlowski, 2003a,b), which made it possible to determine the content of unfrozen loosely bound water.

Certain studies (Kozlowski, 2003a,b) proposed a method for determination of the content of unfrozen water based on the differential scanning calorimetry (DSC) data. As a result, the experimental dependence of the content of unfrozen water on temperature was calculated. Also, the latent heat of fusion was measured for the distilled water, and the results were used to determine the content of unfrozen water in bentonite clay. In the present study, it is shown that with a decrease in the temperature the content of unfrozen water stops changing, and this remaining liquid water is called non-freezing water, because it does not undergo a phase transition.

Previously (Mironov and Lukin, 2011; Mironov and Savin, 2015; Mironov et al., 2017) we proposed to use soil dielectric measurements for quantitative estimation of soil water components, such as tightly bound water, loosely bound water and unbound water in both thawed and frozen soils.

According to the results (Mironov and Lukin, 2011), the dielectric constant of loosely bound water at a frequency of 8 GHz decreased from 90 to 9 when transition from thawed state to frozen state of soil. Taking into account that the permittivity has changed between values close to liquid water and ice, it was suggested in the article (Mironov and Lukin, 2011) that a decrease in the mass of unfrozen (loosely bound) water with a simultaneous increase in ice mass can be attributed to a phase transition of unfrozen (loosely bound) water into ice. At the same time, the approach developed in the article (Mironov and Lukin, 2011) allowed estimating the temperature dependence of the ice mass in frozen soil formed as a result of phase transition at the expense of unfrozen water. However, the change in dielectric permittivity with temperature is not constitute a definitive indication of the presence of a phase transition. Consequently, the issue of application of developed in article (Mironov and Lukin, 2011) methodology based on dielectric permittivity in the examination of phase transition remains inconclusive.

In the present study, we carried out both dielectric and calorimetric measurements on the same bentonite clay and compared the results with the view to evaluate the possibility of analyzing phase transition processes using the dielectric method. The results were used as the basis to develop an interpretation method of dielectric measurements as indicated in the work (Mironov and Lukin, 2011).

2. Soil characteristics. Investigation methods

In order to determine the content of unfrozen water and analyze its phase transition in the frozen soil we chose Na-bentonite clay. The composition of the sample was dominated by montmorillonite, a smectite clay, which made up approximately 70%, quartz which accounted for approximately 15%, carbonates ~3–5 % (tiff + traces of dolomite), feldspar ~3–5 % (sodium-calcium feldspar ~2–3 %, potassium feldspar ~1–2 %), kaolinite ~ 1%, chlorite ~1%, and mica ~1%. The results of the granulometric analysis are indicated in Table 1.

2.1. Calorimetric measurements and preparation of samples

Calorimetric measurements were based on the use of differential scanning calorimeter DSC 204 F-1 Phoenix (NETZSCH, Germany). The measurements were conducted on samples with different moisture content, from 0.139 to 0.69 g/g (20 samples were used) and at temperatures ranging from −40 to 20 °C. Samples were first frozen to −40 °C, after which they were heated at a rate of 5 K/min. Whilst the sample were heated in the calorimeter, the flow of heat absorbed by the soil sample was measured as a function of temperature.

The samples were prepared one time before calorimetric and dielectric measurements. Large lumps of Na-bentonite clay were made homogeneous, using a porcelain pestle and mortar. Equal portions of clay were placed in sample bottles. Using a pipette dispenser, a predetermined content of distilled water was added to each bottle of clay, so as to have an calculated equal moisture distribution from the dry soil to a moisture content of about 70% by mass. Precise moisture of the obtained samples was determined after completion of measurements and drying of the soil samples. The bottles were then hermetically sealed and kept for 7 days at room temperature to allow the moisture in each bottle to spread equally through the sample. Upon expiry of 7 days, the moist samples were placed in an aluminium measuring containers which were sealed using a special press. Before and after the measurements were made, the samples were weighed together with the containers, thus the amount of water that was lost during the measurement was determined. Upon completion of a series of measurements, it was found that the loss of water mass during the measurements (approximately 2.5 h) was equal to null. After the measurements,

Table 1
Grain size composition of Na-bentonite clay.

$d > 0.05$ mm Sand	$0.05 \geq d \geq 0.002$ mm Silt	$d < 0.002$ mm Clay
0.2%	35%	64.8%

the containers with the samples were pierced with a needle and placed in a drying chamber, where they were left for 24 h at a temperature of 104 °C. Once dried up, the samples were weighed again, before any additional moisture could condensate, so that the values obtained indicated the sample weight in the dry condition. After determining the dry mass of the sample m_d, as well as the mass of water added to the sample m_w, the moisture content in the sample was calculated using the following formula: $m_g = m_w/m_d$.

2.2. The dielectric measurement method and processing of the data

The measured soil samples with the prescribed moisture content were placed in a container shaped as a coaxial waveguide. The measured container was manufactured with length of 37 mm, the radius of the cavity of 7 mm, and the radius of the central conductor of 3 mm. Using Agilent vector network analyzer, we measured the amplitudes and phases of the S_{11} and S_{12} components of the scattering matrix within the frequency range from 0.05 to 15 GHz. Based on the described methods (Mironov et al., 2010b, 2013), using the S-elements of the transition matrix, we obtained the frequency spectra of the real and imaginary parts of the complex refractive index (CRI) for bentonite $n_s^* = n_s + i\kappa_s$, where n_s and κ_s are, respectively, the refractive index (RI) and the normalized attenuation coefficient (NAC) of the electromagnetic wave in the examined sample. The CRI is related to complex relative permittivity (CRP) $\varepsilon_s^* = \varepsilon_s' + i\varepsilon_s''$ as follows:

$$n_s^* = n_s + i\kappa_s = \sqrt{\varepsilon_s^*} = \sqrt{\varepsilon_s' + i\varepsilon_s''}, \tag{1}$$

where ε_s' — the dielectric constant of the substance (DC), ε_s'' — the dielectric loss factor (LF). From formula (1) it is easy to obtain the following relations:

$$\varepsilon_s' = n_s^2 - \kappa_s^2, \tag{2}$$

$$\varepsilon_s'' = 2n_s\kappa_s. \tag{3}$$

In order to maintain the set temperature of the sample in a continuous fashion, we used the SU-241 Espec controlled temperature chamber. The accuracy of the temperature settings in the chamber was 0.1 °C. The moment when the temperature of the sample would reach a certain present level, based on the prescribed value, was determined automatically, so that any deviations in temperature due to technological processes in the chamber could be avoided. Furthermore, such automation considerably shortens the time required for controlling the set sequence of temperatures. A detailed description of the method of control of the thermodynamic balance at set temperatures in the heating chamber is provided in the work (Mironov et al., 2010b).

In paper (Shutko and Reutov, 1982) based on the comparison of measured of the CRP of moist soils with the results of calculation of these values, using different dielectric models of the mixture, it was shown that the refractive model, proposed in the work (Birchak et al., 1974), provides the most accurate results in comparison with other models, when defining the dependence in terms of moisture of the real and the imaginary part of the soil's CRP. The refractive model was generalized to account for the fact that the soil may contain different water components such as: tightly bound water, loosely bound water, unbound water and ice (Mironov et al., 2004).

In the case of p-component heterogeneous dielectric mixture, the refractive model can be recorded as follows:

$$\sqrt{\varepsilon_s^*} = \sum_{i=1}^{p} \sqrt{\varepsilon_i^*} = \sum_{i=1}^{p} n_i^* W_i, \tag{4}$$

where ε_i^*, n_i^* — CRP and CRI of the i's mixture component, W_i— relative volumetric fraction of the i's mixture component, determined based on the ratio between the volume of the i's component and the total volume of the mixture:

$$W_i = \frac{V_i}{V}. \tag{5}$$

Obviously, it follows from Eq. (5) that

$$\sum_{i=1}^{p} W_i = 1. \tag{6}$$

According to the concept of classification of types of water in the soil, described in Section 1, the following types of water can be distinguished in thawed soil: 1) tightly bound water, the molecules of which are adsorbed on the surface of mineral particles; 2) loosely bound water, which interacts with molecules of tightly bound water; 3) unbound water, which fills inter-porous space. In frozen soils the entire volume of unbound water as well as part of loosely bound water is transformed into ice, and the other part of loosely bound water together with tightly bound water form the components of unfrozen water. In accordance with the concept discussed above, the refractive model for thawed soil CRI can be written as follows:

$$n_s^* = n_m^* W_m + n_a^* W_a + n_b^* W_b + n_t^* W_t + n_u^* W_u, \tag{7}$$

where indexes m, a, b, t, and u indicate the mineral component, the air component, the tightly bound water, the loosely bound water and the unbound water in thawed soils, respectively. Whilst in the case of frozen soils, Eq. (4) takes the form:

$$n_s^* = n_m^* W_m + n_a^* W_a + n_b^* W_b + n_t^* W_t + n_i^* W_i, \tag{8}$$

where index i indicates ice in frozen soils.

Considering that $\varepsilon_a^* = 1$ and taking into account Eq. (6), we obtained the following equation for thawed soils:

$$n_s^* = n_d^* + (n_b^* - 1)W_b + (n_t^* - 1)W_t + (n_u^* - 1)W_u, \tag{9}$$

and for frozen soils:

$$n_s^* = n_d^* + (n_b^* - 1)W_b + (n_t^* - 1)W_t + (n_i^* - 1)W_i, \tag{10}$$

where

$$n_d^* = (n_m^* - 1)W_m + 1, \tag{11}$$

and where parameter n_d^* corresponding to CRI of dry soil. If we assume that the volume of the soil does not change with the addition or reduction of water content in the mixture, where the water fills the pores, squeezing out the air, the volume of the moist sample is equal to the volume of dry mass and consequently the expression (11) can be rewritten as follows:

$$n_d^* = (n_m^* - 1)\frac{\rho_d}{\rho_m} + 1, \tag{12}$$

where ρ_d and ρ_m— the dry bulk density of soil and the density of the mineral particles, respectively. Eqs. (9) and (10) can also be written in terms of the gravimetric contents of each water component, taking into account the fact that the expression of the volumetric fraction of p's water component (where $p = b,t,u,i$ represents tightly bound, loosely bound, unbound water, and ice, respectively) based on gravimetric value is as follows:

$$W_p = \frac{m_p}{m_d}\frac{\rho_d}{\rho_p} = m_{gp}\frac{\rho_d}{\rho_p}, \tag{13}$$

where

$$m_{gp} = \frac{m_p}{m_d}. \tag{14}$$

As a result, Eqs. (9) and (10) for thawed soils take the form:

$$n_s^* = n_d^* + (n_b^* - 1)m_{gb}\frac{\rho_d}{\rho_b} + (n_t^* - 1)m_{gt}\frac{\rho_d}{\rho_t} + (n_u^* - 1)m_{gu}\frac{\rho_d}{\rho_u}. \tag{15}$$

And those for frozen soils are the following:

$$n_s^* = n_d^* + (n_b^* - 1)m_{gb}\frac{\rho_d}{\rho_b} + (n_t^* - 1)m_{gt}\frac{\rho_d}{\rho_t} + (n_i^* - 1)m_{gi}\frac{\rho_d}{\rho_i}, \quad (16)$$

where ρ_b, ρ_t, ρ_u, ρ_i— density of tightly bound water, loosely bound water, unbound water, and ice, respectively. The moisture m_g is equal to the sum of contents of the water components present in the soil, so that:

$$m_g = m_{gb} + m_{gt} + m_{gu,i}. \quad (17)$$

As can be seen from Fig. 1.4 in Wu et al. (2008), water in thawed soil forms a layered structure, the layer of the molecules closest to the surface of soil particles consists of molecules of tightly bound water, the layer of water adjacent to tightly bound water appears when the moisture content of the sample becomes greater than the maximum possible content of tightly bound water in a given soil m_{g1}. In samples of soil with a moisture content $m_{g1} \le m_g \le m_{g2}$, a loosely bound water layer is formed, where m_{g2} is the maximum possible content of total bound water. With further increase in moisture $m_g > m_{g2}$ the layer of unbound water is formed in the soil. Consequently, three moisture ranges were determined:

1. $m_g \le m_{g1}$, all water is in the tightly bound state,
2. $m_{g1} < m_g \le m_{g2}$, a part of the water ($m_{gb} = m_{g1}$) is in the tightly bound state, whilst the rest of the water ($m_g - m_{g1}$) is in the loosely bound state,
3. $m_g > m_{g2}$, the water in the soil can be found in all three states, where the content of tightly bound water is equal to $m_{gb} = m_{g1}$, the content of loosely bound water is equal to $m_{gt} = m_{g2} - m_{g1}$, whilst the content of the water ($m_g - m_{g2}$) is unbound water in thawed soils or ice in frozen soils.

From Eqs. (12), (15) and (16), it is not difficult to obtain the expression of the refractive dielectric model for the reduced coefficient of RI ($(n_s - 1)/\rho_d$) and NAC (κ_s/ρ_d) as this was done in Mironov et al. (2010a) to provide analysis dielectric experimental data for soil samples, the dry bulk density of which depends on the sample moisture. Based on the foregoing, we can write refractive model as follows:

$$\frac{n_s(m_g, f, T) - 1}{\rho_d(m_g)} = \begin{cases} \dfrac{n_m - 1}{\rho_m} + \dfrac{(n_b(f, T) - 1)}{\rho_b} m_g, & m_g \le m_{g1}, \\ \dfrac{n_m - 1}{\rho_m} + \dfrac{(n_b(f, T) - 1)}{\rho_b} m_{g1} & m_{g1} < m_g \le m_{g2}, \\ \quad + \dfrac{(n_t(f, T) - 1)}{\rho_t}(m_g - m_{g1}), & \\ \dfrac{n_m - 1}{\rho_m} + \dfrac{(n_b(f, T) - 1)}{\rho_b} m_{g1} & \\ \quad + \dfrac{(n_t(f, T) - 1)}{\rho_t}(m_{g2} - m_{g1}) & \\ & m_{g1} < m_g \le m_{g2}, \\ \quad + \dfrac{(n_{u,i}(f, T) - 1)}{\rho_{u,i}}(m_g - m_{g2}), & \end{cases} \quad (18)$$

$$\frac{\kappa_s(m_g, f, T)}{\rho_d(m_g)} = \begin{cases} \dfrac{\kappa_m}{\rho_m} + \dfrac{\kappa_b(f, T)}{\rho_b} m_g, & m_g \le m_{g1}, \\ \dfrac{\kappa_m}{\rho_m} + \dfrac{\kappa_b(f, T)}{\rho_b} m_{g1} + \dfrac{\kappa_t(f, T)}{\rho_t}(m_g & m_{g1} < m_g \le m_{g2}, \\ \quad - m_{g1}), & \\ \dfrac{\kappa_m}{\rho_m} + \dfrac{\kappa_b(f, T)}{\rho_b} m_{g1} + \dfrac{\kappa_t(f, T)}{\rho_t}(m_{g2} & \\ \quad - m_{g1}) & \\ \quad + \dfrac{\kappa_{u,i}(f, T)}{\rho_{u,i}}(m_g & m_{g1} < m_g \le m_{g2}. \\ \quad - m_{g2}), & \end{cases} \quad (19)$$

In formulas (18), (19) the indices of u and i of the values $n_{u,i}$ and $\kappa_{u,i}$ stand for unbound water in the thawed soil and ice in the frozen soil, respectively.

Further, we will analyze the experimental data in the case of frozen soils. The refraction model (Eqs. (18), (19)) makes it possible to find the values of the maximum content of tightly bound water m_{g1}, the total content of bound water m_{g2} and the CRI of each component of soil water in frozen soils. The refractive model (Eqs. (18), (19)), expressed through the values of gravimetric moisture of soil, is the piecewise-linear function, with the slope ratio determined by RI and NAC of the tightly bound water in the given section corresponding to moisture $m_g \le m_{g1}$, the moisture range $m_{g1} < m_g \le m_{g2}$ corresponds to the slope angle tangent determined based on RI and NAC of the loosely bound water, whilst the moisture range $m_g > m_{g2}$ corresponds to ice.

Thus, approximating the measured values of reduced RI and NAC with formulas (18), (19), we can estimate the values of maximum content of tightly bound water m_{g1} and the maximum content of total bound water m_{g2} in frozen soils.

As shown by the analysis of the experimental data, carried out below in Section 3.2, the changes of m_{g1} and m_{g2} in the measured frequency range do not exceed errors of the single frequency estimations for m_{g1} and m_{g2}. Therefore, further we will assume that the frequency dependence for the values of m_{g1} and m_{g2} is absent, and we can find the average values for the frequency range of measurements of the values of m_{g1} and m_{g2} using the refraction model averaged over frequencies as follows:

$$\left\langle \frac{n_s - 1}{\rho_d} \right\rangle = \begin{cases} \left\langle \dfrac{n_m - 1}{\rho_m} \right\rangle + \left\langle \dfrac{(n_b - 1)}{\rho_b} \right\rangle m_g, & m_g \le m_{g1}, \\ \left\langle \dfrac{n_m - 1}{\rho_m} \right\rangle + \left\langle \dfrac{(n_b - 1)}{\rho_b} \right\rangle m_{g1} & m_{g1} < m_g \\ \quad + \left\langle \dfrac{(n_t - 1)}{\rho_t} \right\rangle (m_g - m_{g1}), & \le m_{g2}, \\ \left\langle \dfrac{n_m - 1}{\rho_m} \right\rangle + \left\langle \dfrac{(n_b - 1)}{\rho_b} \right\rangle m_{g1} & \\ \quad + \left\langle \dfrac{(n_t - 1)}{\rho_t} \right\rangle (m_{g2} - m_{g1}) & \\ \quad + \left\langle \dfrac{(n_{u,i} - 1)}{\rho_{u,i}} \right\rangle (m_g & m_{g1} < m_g \\ \quad - m_{g2}), & \le m_{g2}, \end{cases} \quad (20)$$

$$\left\langle \frac{\kappa_s}{\rho_d} \right\rangle = \begin{cases} \left\langle \frac{\kappa_m}{\rho_m} \right\rangle + \left\langle \frac{\kappa_b}{\rho_b} \right\rangle m_g, & m_g \le m_{g1}, \\ \left\langle \frac{\kappa_m}{\rho_m} \right\rangle + \left\langle \frac{\kappa_b}{\rho_b} \right\rangle m_{g1} + \left\langle \frac{\kappa_t}{\rho_t} \right\rangle (m_g - m_{g1}), & m_{g1} < m_g \le m_{g2}, \\ \left\langle \frac{\kappa_m}{\rho_m} \right\rangle + \left\langle \frac{\kappa_b}{\rho_b} \right\rangle m_{g1} + \left\langle \frac{\kappa_t}{\rho_t} \right\rangle (m_{g2} - m_{g1}) & \\ \quad + \left\langle \frac{\kappa_{u,i}}{\rho_{u,i}} \right\rangle (m_g - m_{g2}), & m_{g1} < m_g \le m_{g2}, \end{cases} \tag{21}$$

where the values indicated in pointed brackets have been averaged based on their frequencies, so that for the n-time measured value Φ:

$$\langle \Phi \rangle = \frac{\sum_{i=1}^{n} \Phi}{n}.$$

3. Results and analysis

3.1. Calorimetric investigation

Calorimetric investigation allowed us to record the DSC signals for samples with a different moisture content. As an example, Fig. 1 illustrates the values of DSC signals whilst the samples were heated. We can see on the figure that with an increase in the moisture content, the amount of absorbed heat in the sample also increases. It is seen from Fig. 1 that the heat is absorbed at all moistures except for $m_g = 0.146$ g/g, which indicates present of water phase transition at these moistures.

In order to determine in what moisture range the phase transition is not observed, we measured samples containing: $m_g = 0.139$ g/g, $m_g = 0.146$ g/g, $m_g = 0.155$ g/g. For moisture contents lower than a value close to $m_g = 0.155$ g/g heat has not been absorbed, so it was noted that phase transition does not occur. It can be observed on Fig. 2 where the volume of absorbed heat is indicated for different moisture content of the samples. Measurement results in Fig. 2 make it possible to determine the maximum value of moisture, at which samples contain only non-freezing water. In order to achieve this result, we applied an approximation in the form of a piecewise-linear dependence to the measurement results, as illustrated in Fig. 2. This figure shows that there is a point which distinguishes samples in which heat is not absorbed from those where it is. This point, indicated as $m_{gt} = 0.166$ g/g, represents the maximum gravimetric moisture below which water in the sample does not undergo a phase transition. The phase transition of ice into unfrozen water in the measured bentonite clay is observed at sample moistures $m_g > m_{gt}$. At that, the amount of absorbed heat is proportional to the excess of moisture of a given sample over the maximum gravimetric moisture below which water in the sample does not undergo a phase transition. Consequently, where sample moisture is less than 0.166 g/g, the sample contains only non-freezing water in the measured range of temperatures.

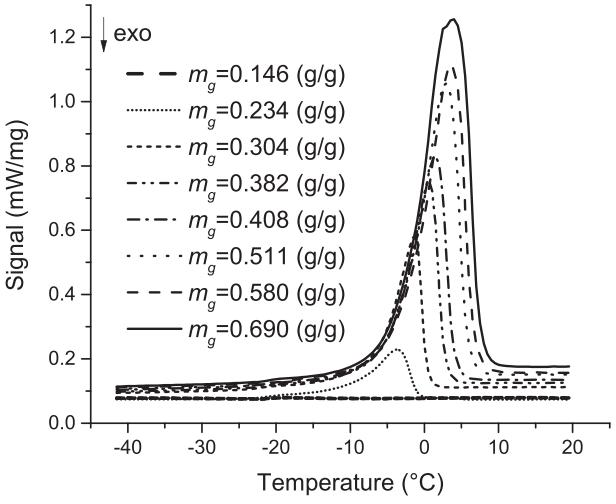

Fig. 1. The endothermic signal peak for Na-bentonite clay samples of different moisture, depending on the temperature.

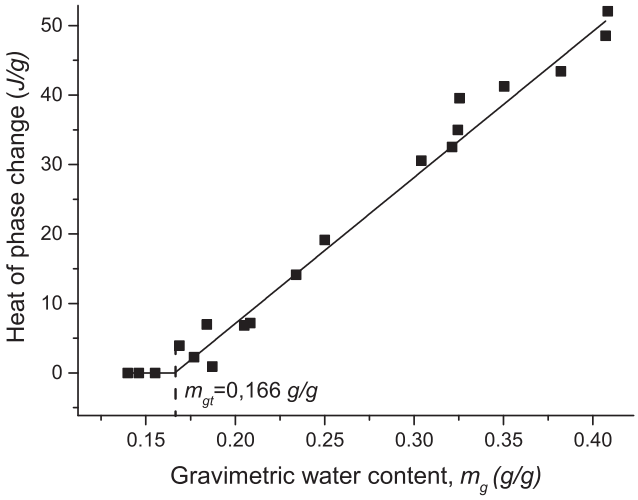

Fig. 2. The absorbed heat of phase transition in soil, depending on sample moisture.

Thus, based on the results illustrated in Fig. 2, only the water corresponding the excess of sample moisture over the maximum content of non-freezing water $m_{gt} = 0.166$ g/g undergoes phase transitions of ice into unfrozen water. Once we know the maximum moisture content, below which the water in the samples does not undergo a phase transition, we can calculate the mass of water present in the sample Δm_w, which will undergo a phase transition, based on the following formula:

$$\Delta m_w = (m_g - m_{gt}) m_d, \tag{22}$$

where m_d— the mass of the dry sample (g), m_g— the total moisture content in the sample in (g/g). By applying formula (22), we can calculate the dependence of the heat, absorbed as a result of the phase transition, on the mass of water Δm_w, undergoing the phase transition at different soil moisture. This dependence is illustrated in Fig. 3.

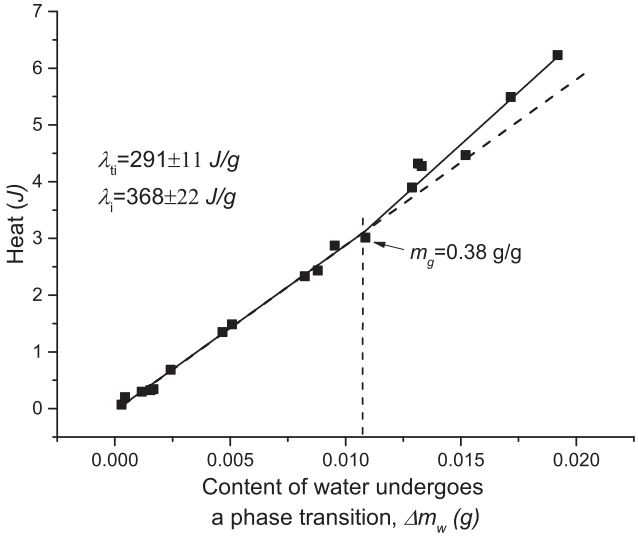

Fig. 3. Dependence of the heat, absorbed by water during the phase transition, on the mass of water.

The measured data for the heat, absorbed from water during the phase transition, indicated in Fig. 3 can be easily approximated using a piecewise-linear function. The slope angle tangents of the piecewise line are equal to the values of latent heat of fusion $\lambda_{ti} = 291 \pm 11$ J/g, $\lambda_i = 368 \pm 22$ J/g, which could be related to phase transitions of ice into different unfrozen water components. We know that when moisture do not exceed the value of some threshold, the soil water remains in bound state, and that with further increase in the moisture content beyond this threshold an additional content of water is found to be in the unbound state (Wu et al., 2008). Consequently, we can assume that the established value λ_{ti} represents latent heat of fusion due to the phase transition of ice into unfrozen bound water, whilst λ_i represents the latent heat of fusion caused by the transition of ice into liquid unbound water.

Consequently, conducting measurements on the samples of the different moistures with the use of DSC allowed us to suppose that, within the gravimetric moisture range from 0.166 to 0.38 g/g we observed the phase transition of ice into unfrozen bound water and, where the gravimetric moisture exceeds 0.38 g/g, we observed an additional phase transition of ice into unbound water. Keeping this in mind, we can consider the value of moisture $m_g = 0.38$ g/g as the maximum content of unfrozen bound water arising due to phase transition of soil water. Furthermore, the following phase transition parameters could be determined: the maximum content of non-freezing water, the maximum content of unfrozen bound water, as well as values relative to latent heat corresponding to the transition of ice into unfrozen bound soil water and to the transition of ice into unfrozen unbound soil water. Previously, calorimetric testing was not conducted on samples with a set moisture content (Kozlowski, 2003a,b; Kozlowski and Nartowska, 2013).

The dependence of the content of unfrozen water on temperature is an important feature of frozen soils (Williams, 1964; Kozlowski, 2003a,b; Kozlowski and Nartowska, 2013). In order to evaluate the dependence of the content of unfrozen water on temperature, the following experiment was conducted. The heat absorbed by the moist samples was measured in the following sequence of temperature settings: [−40 °C, −15 °C], [−40 °C, −10 °C], [−40 °C, −7 °C], [−40 °C, −5 °C], [−40 °C, −4 °C], [−40 °C, −3 °C], [−40 °C, −2 °C]. The sample with the moisture content of $m_g = 0.66$ g/g was frozen to $T = -40$ °C, then the same sample was heated to $T = -15$ °C and it was maintained at this constant temperature for 10 min. The sample was then frozen again to $T = -40$ °C, and then reheated to $T = -10$ °C and this temperature was maintained for 10 min. A similar experiment was conducted at temperatures of − 7 °C, − 5 °C, − 4 °C, − 3 °C, − 2 °C. Furthermore, the amount of heat absorbed in each cycle of heating was also recorded.

Knowing the overall amount of heat Δh, which is absorbed in each measured temperature range (see Fig. 4), we can calculate the content of unfrozen water m_{gu} (g/g), generated by phase transition, as follows:

$$m_{gu} = \frac{\Delta h}{\lambda_{ti} m_d} + m_{gt}. \quad (23)$$

Fig. 4 shows that DSC signals, obtained when a set negative temperature is reached, coincide to the DSC signal obtained for a complete thawing cycle, from −40 to 20 °C. Consequently, it can be concluded that this type of experiment is not essential, since each individual DSC signal with narrower temperature interval, can be reproduced as a part of a broader DSC signal corresponding to this narrow temperature interval. A similar method was used by Horiguchi (1985). The present study confirms this approach (Horiguchi, 1985) through experiments.

The results pertaining to the content of unfrozen water depending on temperature, obtained from this experiment are indicated in Fig. 5. As shown in Fig. 5 an increase in the temperature brings about an increase in the content of unfrozen water in accordance with a certain non-linear dependence. When calculating the content of unfrozen water, which is shown in Fig. 5, we used the value of latent heat of fusion, assuming that all unfrozen water is in a bound state at temperatures $T < 0$ °C. By comparing the results pertaining to the content of unfrozen water, obtained in work (Kozlowski and Nartowska, 2013), which uses Na-bentonite clay, and our results, we calculated the normalized standard deviation, which was 20.8% of the data in Kozlowski and Nartowska (2013) from those obtained by us. The estimated divergences were observed most likely due to the measured samples were not identical to each other.

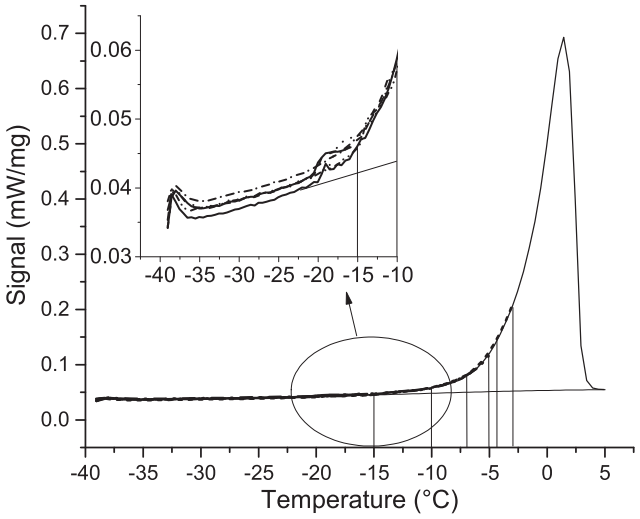

Fig. 4. The dependences of the DSC signals of the heat cycles on the temperature.

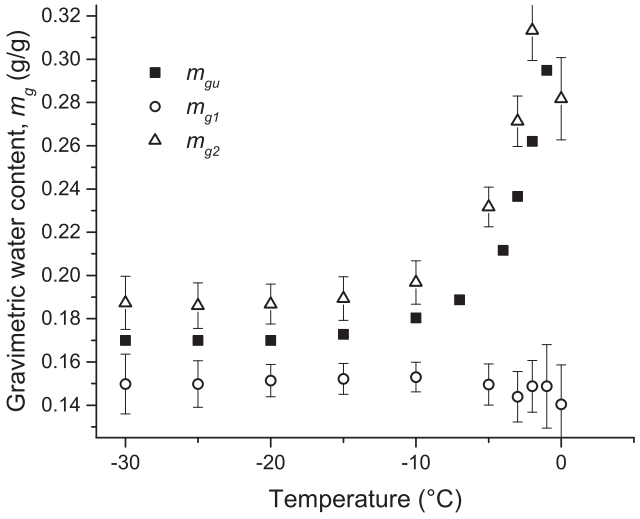

Fig. 5. The dependence of the maximum content of the tightly bound water on temperature m_{g1}, and that of the maximum content of the total bound water m_{g2}, as determined by the dielectric method, and the content of unfrozen water, m_u, as determined by the calorimetric method.

3.2. Dielectric investigation

During the calorimetric tests we defined the temperature dependence of the mass of unfrozen water, produced by phase transition. Furthermore, the variations in the content of unfrozen loosely bound water with temperature can be obtained by dielectric measurements. This is why we conducted the measurement of RI and NAC of Na-bentonite clay in the frequency range of electromagnetic wave from 0.05 to 15 GHz, by heating the samples from −30 to 0 °C.

Next, we analyze the frequency dependences of the values of m_{g1}

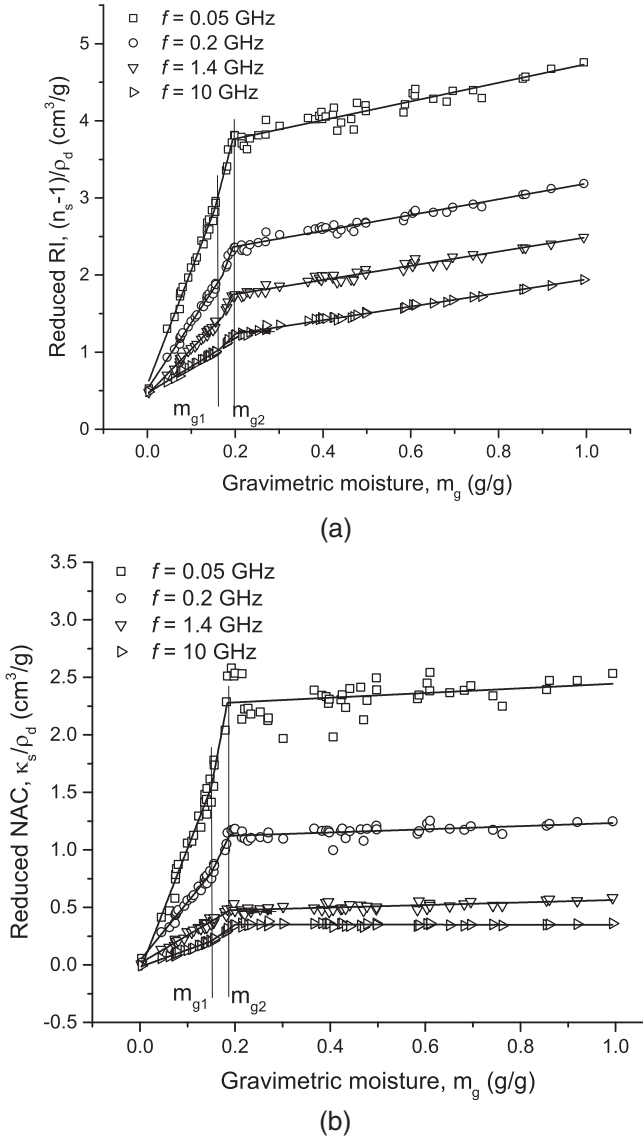

Fig. 6. The reduced RI, $(n_s - 1)/\rho_d$ (a), and NAC, κ_s/ρ_d (b), as a function of gravimetric moisture, as measured at several frequencies at a temperature $T = -10$ °C.

and m_{g2} in the frequency range of measurements. As an example, Fig. 6 demonstrates reduced RI and NAC of Na-bentonite as a function of the gravimetric moisture as measured at several frequencies at a temperature of $T = -10$ °C, as well as the results of approximation lines with the use of formulas (18) and (19).

The frequency dependences of the values of the maximum content of unfrozen tightly bound water m_{g1} and the maximum content of total bound water (the total content of unfrozen water found by the dielectric method) m_{g2} for all measuring frequencies at a temperature $T = -10$ °C are shown in Fig. 7. Also the measurement errors of m_{g1} and m_{g2} are given in Fig. 7. It is seen from Fig. 7 that the changes in m_{g1} and m_{g2} in the whole range of measured frequencies are within the limits of their estimation errors. Thus, assuming that the values of m_{g1} and m_{g2} are independent of frequency, we can use formulas (20) and (21) for the estimation of their values in the whole measured frequency range. For the other measured temperatures, the averaged Eqs. (20) and (21) can also be applied. In the further estimates of m_{g1} and m_{g2} we will use, averaged over frequency, Eqs. (20) and (21).

Fig. 8 contains symbols representing values depending on their moisture content for the results of measurements of the reduced RI and

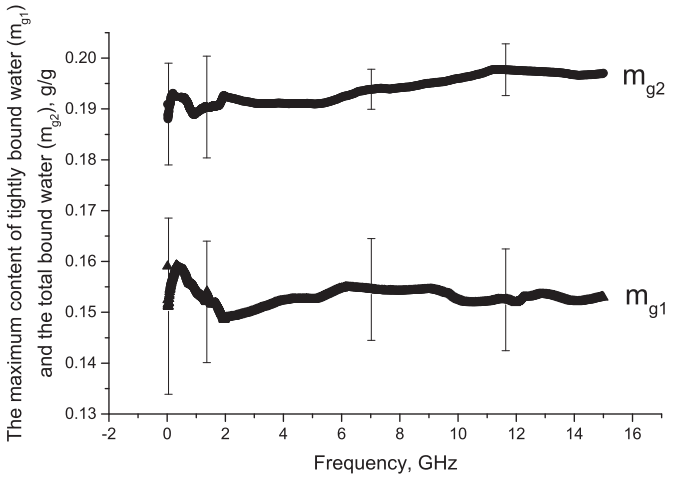

Fig. 7. The maximum content of tightly bound water m_{g1} and the maximum content of total bound water m_{g2} as a function of frequency at a temperature of $T = -10$ °C.

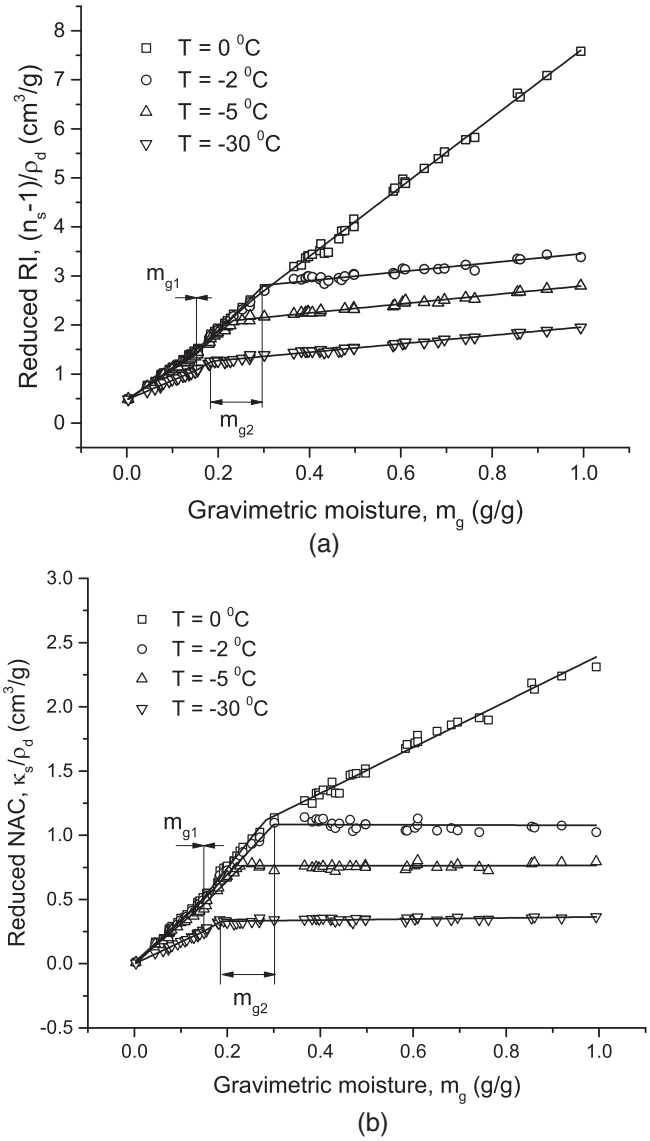

Fig. 8. The reduced RI, $(n_s - 1)/\rho_d$ (a), and NAC, κ_s/ρ_d (b), as a function of gravimetric moisture, as measured at several temperatures, obtained in the runs of heating.

NAC of bentonite, averaged over the measurement frequency range from 0.05 to 15 GHz, with the average measured frequency being equal to 4.6 GHz, at several temperatures. Solid lines indicate results of approximation, based on the formulas (20) and (21). We note that the experimental data indicated for RI and NAC Na-bentonite can be well represented by a piecewise-linear function of moisture with three linear sections, distinguished from one another by transitional values m_{g1} and m_{g2}. Furthermore, each section of the piecewise-linear function can be linked to an individual soil water component. Further analysis was conducted in the temperature range $T < 0$ °C. As indicated in Fig. 8, within the moisture range $m_g > m_{g2}$, the inclination of the corresponding section is little dependent on temperature, whilst the water RI corresponding to the slope has the value of 1.9 ± 0.1 nearing the value of ice RI, which is 1.73 in the examined frequency range. Thus, we can conclude that this section of the piecewise-linear function corresponds to the soil water components representing ice. In the case of range of moistures of $m_{g1} < m_g < m_{g2}$ the slopes of the reduced RI and NAC become considerably larger then those corresponding to the ice and these values increase with the temperature. In addition, the values of RI and NAC estimated from the expected slopes were found to be close to the respective values corresponding to the loosely bound water in the thawed soil. For instance, the values of RI and NAC, found from the inclination tangents of the respective linear section in the range of moistures of $m_{g1} < m_g < m_{g2}$ at the temperature $T = -10$ °C, are equal to 10.3 ± 0.6 and 3.7 ± 0.3, respectively, whilst the respective values for the RI and NAC estimated at the temperature of $T = 0$ °C are equal to 10.3 ± 0.2 and 5.8 ± 0.2, respectively. Consequently, we can conclude that the given section of piecewise-linear dependencies of the reduced RI and NAC can be attributed to the unfrozen loosely bound water. At the same time, the values of the reduced RI and NAC, estimated in the same way in the range of moistures of $m_g < m_{g1}$, were found to be larger than those corresponding to ice and smaller than the ones corresponding to the unfrozen loosely bound water. In addition, they appeared to be closed to the values corresponding to the tightly bound water in the thawed soil (at $T = -10$ °C the RI is equal to 6.7 ± 0.1, the NAC is equal to 2.7 ± 0.1; at $T = 0$ °C the RI is equal to 8.9 ± 0.3 and the NAC is equal to 4.3 ± 0.3).

Fig. 5 shows the maximum content of tightly bound water (m_{g1}) and the maximum content of total bound water (m_{g2}) depending on the temperature. The value of m_{g2} represents the maximum content of unfrozen water in the soil, determined from the dielectric measurements. In the same figure the total content of unfrozen water is given as determined by DSC measurements. It is also seen from Fig. 5 that the value of the maximum content of tightly bound water remains unchanged in the whole range of measured temperatures. Consequently, we can conclude that there is no mass exchange between tightly bound water and the other water components in the frozen soils when the temperature changes. Therefore, all the content of unfrozen tightly bound water must be classified as non-freezing water, which does not participate in the phase transition process. In the temperature range from −30 to − 20 °C the dependence of m_{g2} on the temperature undergoes saturation, approaching the value $m_{g2} = 0.19$. This indicates gradual termination of mass exchange between ice and unfrozen bound water. Therefore, the value of $m_{g2} = 0.19$ in the temperature range from −30 to − 20 °C can be defined as the maximum content of non-freezing water found by the dielectric method, in further this value will be denoted as m_{g2nz}. Thus, non-freezing water in the frozen soils in the whole measured temperature range, as it shown in Fig. 5, consist of the non-freezing tightly bound water in the content of $m_{g1} = 0.15$ g/g and the non-freezing loosely bound water in the content of $m_{g2nz} - m_{g1} = 0.19 - 0.15 = 0.04$ g/g. In the temperature range from −20 to 0 °C the content of unfrozen total bound water m_{g2} increases almost two time as the expense of ice decreasing. At that, the content of water, which has arisen due to the melting of ice, is equal to ($m_{g2} - m_{g2nz}$), and this part of water should be referred to the unfrozen loosely bound water. From Fig. 5, it can be seen that the values of the maximum content of unfrozen water derived from applying the dielectric method (m_{g2}), on the one hand, and the calorimetric method (m_{gu}), on the other hand, are in a good agreement with which other, whilst the root mean standard deviation of m_{g2} from the value of m_{gu} is $RMSD = 0.026$, and the determination coefficient is $R^2 = 0.71$. Since the calorimetric method measures the absorbed heat, which is recalculated in the content of thawed water, then, by its nature, it detects namely unfrozen water. Moreover, since the mass of this water coincides with the value found from the dielectric measurements, then the maximum content of total bound water m_{g2} corresponds to unfrozen water either. The small difference observed between the values measured by the dielectric and the DSC methods can be explained by the fact that the dry bulk densities of the samples at the same moisture differed from each other. It takes place because in accordance with the dielectric measurement procedure, the soil substance of samples is especially pressed (see Mironov et al., 2017), whilst such pressing is not applied in the calorimetric measurements.

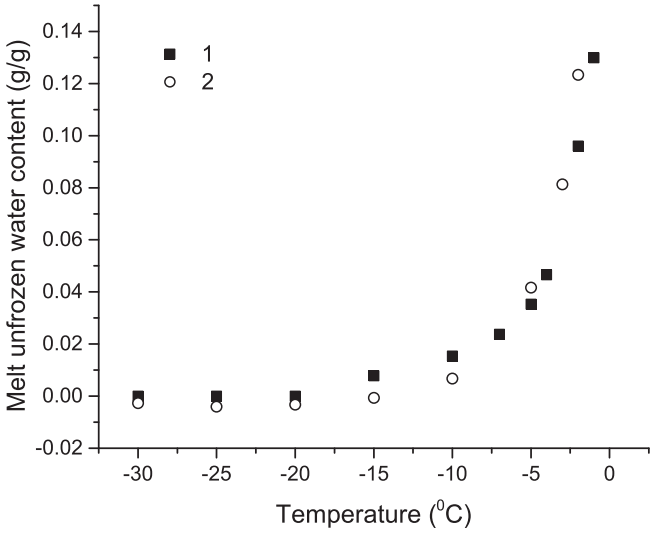

Fig. 9. The temperature dependencies of the content of water arising due to ice melting, found by two different methods — dielectric *(1)* and calorimetric *(2)*.

Fig. 9 shows the increments in unfrozen water content arising due to ice melting found by two different methods — calorimetric and dielectric. The degree of good consistency between these increments is characterized by the estimated value of the root mean square deviation of one from the other, which is equal to 0.01, and the respective determination coefficient was estimated as 0.93. This good consistency confirms possibility to use the proposed dielectric method for estimating the mass of liquid water in soil arising as a result of phase transition of ice. As a result in this research, there was proposed a possibility to estimate the value of heat absorbed in the process of ice phase transition into unfrozen water in the soil, on the basis of the unfrozen water increments derived with the use of the proposed dielectric method and the value of latent heat of fusion concerning phase transition of ice into unfrozen water derived with the use of the proposed modification in the calorimetric method.

When estimating the latent heat of fusion (see Section 3.1), it was assumed that all unfrozen water detected in calorimetric measurements can be classified as unfrozen bound water. Such an assumption can be justified by the good agreement between the maximum content of total bound water measured by the dielectric method and the content of unfrozen water measured by the calorimetric method, which is discussed above.

4. Conclusions

Our investigation of the phase transitions of water in Na-bentonite

clay, using the DSC method, in the temperature range from −40 to 20 °C identified the following water components found in frozen soil: non-freezing water, unfrozen water and ice. The study proposes estimation method for each of these components. As a result, the temperature dependencies linked to the increases in the mass of unfrozen water and the corresponding decrease in the mass of ice were also defined. These dependencies represent phase transitions of water which occur with increasing temperature. Furthermore, using the data obtained by DSC measurements, in the temperature range from −40 to 20 °C we estimated the value of latent heat of fusion in two cases, namely: when ice is transformed into unfrozen bound soil water ($\lambda_{ti} = 291 \pm 11$ J/g), and when ice is transformed into liquid unbound soil water ($\lambda_i = 368 \pm 22$ J/g).

Using the same Na-bentonite clay, in the temperature range from −30 to 0 °C and a gravimetric moisture range from the dry soil to 1 g/g, we measured complex permittivity as a function of temperature and moisture of the soil. Using the results of dielectric measurements, we identified the following water components in frozen soil: non-freezing tightly bound water, non-freezing loosely bound water, unfrozen loosely bound water and ice. We also developed a method to determine the mass of non-freezing tightly bound water, unfrozen loosely bound water and ice. Using this method, we calculated the temperature dependencies of the mass for each aforementioned soil water component. The temperature dependency of the mass of unfrozen loosely bound water, calculated based on DSC measurements, indicates solid quantitative correspondence to the dependencies calculated using dielectric measurement data ($RMSD = 0.026$, $R^2 = 0.71$).

As a result, it was proven that temperature dependence of the mass of loosely bound water as determined by dielectric measurements, is a consequence of the phase transition and can be used to define the characteristics of the phase transition of ice to unfrozen bound water.

It is worth noting that some phenomena that might have been observed during the phase transition of water in Na-bentonite clay are not considered. First, the phenomenon of percolation was not considered, because samples with large water content and at positive temperatures were not measured. Second, in this paper the influence of salts, that complicates the picture of phase transitions at the eutectic points, was not studied. Third, only the process of ice melting in the soil are considered (the reverse process proceeds in a different way).

Acknowledgments

The authors are sincerely grateful to the reviewers for their concerned analyses of the content of this paper and providing the valuable helpful discussion that allowed us to introduce many principle improvements in the text of the manuscript.

This work was supported by Programs II.12.1. Fundamental Research SB RAS, Russia.

References

Birchak, J.R., Gardner, C.G., Hipp, J.E., Victor, J.M., 1974. High dielectric constant microwave probes for sensing soil moisture. Proc. IEEE 62 (1), 93–98.

Bogdan, A., Kulmala, M., Gorbunov, B., Kruppa, A., 1996. NMR study of phase transitions in pure water and binary H_2O/HNO_3 films adsorbed on surface of pyrogenic silica. J. Colloid Interface Sci. 177 (1), 79–87. http://www.sciencedirect.com/science/article/pii/S0021979796900089.

Fabbri, A., Fen-Chong, T., Azouni, A., Thimus, J.-F., 2009. Investigation of water to ice phase change in porous media by ultrasonic and dielectric measurements. J. Cold Reg. Eng. 23 (2), 69–90.

Fabbri, A., Fen-Chong, T., Coussy, O., 2006. Dielectric capacity, liquid water content, and pore structure of thawing-freezing materials. J. Cold Reg. Eng. 44 (1), 52–66. http://www.sciencedirect.com/science/article/pii/S0165232X05000947.

Frivik, P.E., Johansen, H., 1978. Calorimetric Measurements of the Specific Heat and Unfrozen Water for Mineral Types of Soil and Organic Materials. Hanover, N H, U.S. Army Cold Regions Research and Engineering Laboratory.

Frolov, A.D., 1998. Electric and Elastic Properties of Frozen Earth Materials. ONTI PNC Russian Academy of Science Press, Pushchino.

Gun'ko, V., Turov, V., Kozynchenko, O., Palijczuk, D., Szmigielski, R., Kerus, S., Borysenko, M., Pakhlov, E., Gorbik, P., 2008. Characteristics of adsorption phase with water/organic mixtures at a surface of activated carbons possessing intraparticle and textural porosities. Appl. Surf. Sci. 254 (10), 3220–3231. http://www.sciencedirect.com/science/article/pii/S0169433207015711.

He, H., Dyck, M., 2013. Application of multiphase dielectric mixing models for understanding the effective dielectric permittivity of frozen soils. Vadose Zone J. 12 (1).

He, H., Dyck, M., Zhao, Y., Si, B., Jin, H., Zhang, T., Lv, J., Wang, J., 2016. Evaluation of five composite dielectric mixing models for understanding relationships between effective permittivity and unfrozen water content. Cold Reg. Sci. Technol. 130, 33–42. http://www.sciencedirect.com/science/article/pii/S0165232X16301240.

Horiguchi, K., 1985. Determination of unfrozen water content by DSC. In: Proc. 4th Int. Symp. Ground Freezing, Sapporo. vol. 1. pp. 33–38.

Kozlowski, T., 2003a. A comprehensive method of determining the soil unfrozen water curves: 1. Application of the term of convolution. Cold Reg. Sci. Technol. 36 (1-3), 71–79. http://www.sciencedirect.com/science/article/pii/S0165232X03000077.

Kozlowski, T., 2003b. A comprehensive method of determining the soil unfrozen water curves: 2. Stages of the phase change process in frozen soil-water system. Cold Reg. Sci. Technol. 36 (1-3), 81–92. http://www.sciencedirect.com/science/article/pii/S0165232X03000065.

Kozlowski, T., 2007. A semi-empirical model for phase composition of water in clay-water systems. Cold Reg. Sci. Technol. 49 (3), 226–236. http://www.sciencedirect.com/science/article/pii/S0165232X07000729.

Kozlowski, T., 2011. Low temperature exothermic effects on cooling of homoionic clays. Cold Reg. Sci. Technol. 68 (3), 139–149. http://www.sciencedirect.com/science/article/pii/S0165232X11001042.

Kozlowski, T., Nartowska, E., 2013. Unfrozen water content in representative bentonites of different origin subjected to cyclic freezing and thawing. Vadose Zone J. 12 (1).

Mironov, V.L., De Roo, R.D., Savin, I.V., 2010a. Temperature-dependable microwave dielectric model for an Arctic soil. IEEE Trans. Geosci. Remote Sens. 48 (6), 2544–2556.

Mironov, V.L., Dobson, M.C., Kaupp, V.H., Komarov, S.A., Kleshchenko, V.N., 2004. Generalized refractive mixing dielectric model for moist soils. IEEE Trans. Geosci. Remote Sens. 42 (4), 773–785.

Mironov, V.L., Komarov, S.A., Lukin, Y.I., Shatov, D.S., 2010b. A technique for measuring the frequency spectrum of the complex permittivity of soil. J. Commun. Technol. Electron. 55 (12), 1368–1373. http://dx.doi.org/10.1134/S1064226910120065.

Mironov, V.L., Kosolapova, L.G., Lukin, Y.I., Karavaysky, A.Y., Molostov, I.P., 2017. Temperature- and texture-dependent dielectric model for frozen and thawed mineral soils at a frequency of 1.4 GHz. Remote Sens. Environ. 200, 240–249. http://www.sciencedirect.com/science/article/pii/S0034425717303590.

Mironov, V.L., Lukin, Y.I., 2011. A physical model of dielectric spectra of thawed and frozen bentonitic clay within the frequency range from 1 to 15 GHz. Russ. Phys. J. 53 (9), 956–963. http://dx.doi.org/10.1007/s11182-011-9516-4.

Mironov, V.L., Molostov, I.P., Lukin, Y.I., Karavaisky, A.Y., 2013. Method of retrieving permittivity from S_{12} element of the waveguide scattering matrix. In: 2013 International Siberian Conference on Control and Communications (SIBCON), pp. 1–3.

Mironov, V.L., Savin, I.V., 2015. A temperature-dependent multi-relaxation spectroscopic dielectric model for thawed and frozen organic soil at 0.05–15 GHz. Phys. Chem. Earth A/B/C 83-84, 57–64. http://www.sciencedirect.com/science/article/pii/S1474706515000224 Emerging science and applications with microwave remote sensing data.

Osipov, V.I., 2012. Nanofilms of adsorbed water in clay: mechanism of formation and properties. Water Resour. 39 (7), 709.

Shutko, A.M., Reutov, E.M., 1982. Mixture formulas applied in estimation of dielectric and radiative characteristics of soils and grounds at microwave frequencies. IEEE Trans. Geosci. Remote Sens. GE-20 (1), 29–32.

Tsytovich, N.A., 1975. Mechanics of Frozen Ground. Scripta Book Co.

Turov, V., Leboda, R., 1999. Application of 1H NMR spectroscopy method for determination of characteristics of thin layers of water adsorbed on the surface of dispersed and porous adsorbents. Adv. Colloid Interf. Sci. 79 (2), 173–211. http://www.sciencedirect.com/science/article/pii/S0001868697000365.

Watanabe, K., Mizoguchi, M., 2002. Amount of unfrozen water in frozen porous media saturated with solution. Cold Reg. Sci. Technol. 34 (2), 103–110. http://www.sciencedirect.com/science/article/pii/S0165232X01000635.

Williams, P.J., 1964. Unfrozen water content of frozen soils and soil moisture suction. Geotechnique 14 (3), 231–246.

Wu, A., Sun, Y., Liu, X., 2008. Granular Dynamic Theory and Its Applications. Springer Berlin Heidelberg.

Yershov, E.D., Williams, P.J., 2004. General Geocryology. Cambridge university press.